Lithos 119 (2010) 10–19

Contents lists available at ScienceDirect

Lithos

journal homepage: www.elsevier.com/locate/lithos

The Guadalupian–Lopingian boundary mudstones at Chaotian (SW China) are clastic rocks rather than acidic tuffs: Implication for a temporal coincidence between the end-Guadalupian mass extinction and the Emeishan volcanism

Bin He [a], Yi-Gang Xu [a,*], Yu-Ting Zhong [a,b], Jun-Peng Guan [a,b]

[a] Key Laboratory of Isotope Geochronology and Geochemistry, Guangzhou Institute of Geochemistry, Chinese Academy of Sciences, Guangzhou, 510640, China
[b] Graduate University of Chinese Academy of Sciences, Beijing, China

ARTICLE INFO

Article history:
Received 31 October 2009
Accepted 6 June 2010
Available online 12 June 2010

Keywords:
Geochemistry
Mineralogy
XRD
Mudstone, Chaotian
The ELIP, end-Guadalupian mass extinction

ABSTRACT

Previous studies on the temporal link between the end-Guadalupian mass extinction event and Emeishan flood volcanism were mainly based on geochronological and bio- and chemostratigraphic correlation techniques (Wignall et al., 2009). The absence of material-based hard evidence that directly links the extinction with the Emeishan volcanism remains a major obstacle regardless of the indication of coincidence in timing (Isozaki et al., 2007). The Emeishan basalts overlie Permian platform carbonates that may contain a record of the end-Guadalupian mass extinction and erosional product of this province. This paper presents mineralogy and geochemistry of mudstones from the Guadalupian–Lopingian Boundary (G–LB) at Chaotian, SW China. Results indicate that these G–LB mudstones are not air-fall acidic tuff as previously thought, but likely represent clastic rocks derived from erosional deposits of the Emeishan large igneous province (ELIP). Mudstones of the lower part (Group 1) have a geochemical affinity to the Emeishan felsic volcanic rocks, whereas mudstones of the upper part (Group 2) are compositionally akin to mafic components of the Emeishan traps. This chemostratigraphic sequence resembles the Xuanwei Formation which sits on the Emeishan basalts (He et al., 2007). These data therefore indicate that the lower part of the mudstones at the Chaotian G–LB section, the lowermost part of Xuanwei and Longtan Formations and the Emeishan felsic extrusives broadly constitute an isochron horizon throughout the ELIP and adjacent region, suggesting a short duration for the Emeishan volcanism. A temporal coincidence between Emeishan volcanism and the end-Guadalupian mass extinction are therefore inferred thus providing support for a cause-and-effect relationship.

1. Introduction

The temporal link between mass extinction events and large igneous province (LIP) volcanism is one of the most intriguing relationships in Earth's history (Courtillot et al., 1999; Wignall, 2001), with the end-Permian extinction–Siberian Traps association being the most examined (Wignall et al., 2009). In recent years the end-Guadalupian event, at the Middle–Late Permian boundary, has become a subject of great interest. Based on stratigraphic constraints, Courtillot et al. (1999) and Hallam and Wignall (1999) independently proposed that the end-Guadalupian mass extinction coincided with the ELIP in SW China. This notion gained support from a number of geochronological data from mafic dykes (Zhou et al., 2002; Guo et al., 2004; Zhong and Zhu, 2006), mafic lavas (Fan et al., 2004), felsic and alkaline intrusives (Zhong et al., 2007; Luo et al., 2007; Xu et al., 2008) and felsic extrusives and their erosional products (He et al., 2007). However, the temporal link between the end-Guadalupian mass extinction and the ELIP is still a matter of debate (Ali et al., 2005). Former geochronological correlation techniques with inherent timing inaccuracies make this link uncertain (Isozaki and Ota, 2007; Wignall et al., 2009). Secondly, this absence of material-based hard evidence that directly links the extinction with the LIP volcanism remains a major obstacle regardless of the credibility of the coincidence in timing (Isozaki et al., 2007, Isozaki and Ota, 2007). Isozaki's group recently argued, based on the study of the Guadalupian–Lopingian Boundary (G–LB) mudstones and its regional correlation, that the Emeishan flood volcanism *postdated* the end-Guadalupian mass extinction (Ota and Isozaki, 2006; Isozaki et al., 2007; Isozaki, 2007; Isozaki and Ota, 2007). One key point for this argument is the interpretation of an altered, acidic volcanic ash layer as the origin for the G–LB mudstones (Isozaki et al., 2004). However firm evidence has not yet been demonstrated. The ELIP in southwest China was emplaced on a Permian carbonate platform, which may have preserved the marine bio-extinction record and the erosional products of the ELIP. Sections of the platform along the margins of the ELIP thus may provide an opportunity to evaluate the temporal relationship between the extinction and the Emeishan volcanism. To clarify these relations, we have examined the mineralogy and geochemistry of mudstones at Chaotian

* Corresponding author.
E-mail address: yigangxu@gig.ac.cn (Y.-G. Xu).

0024-4937/$ – see front matter © 2010 Elsevier B.V. All rights reserved.
doi:10.1016/j.lithos.2010.06.001

section in the north of the ELIP (Fig. 1). Together with a previous study on the Xuanwei Formation and the uppermost felsic volcanic rocks of the Emeishan succession, we are able to document multiple phenomena associated with the end-Guadalupian mass extinction.

2. Geological background and sampling

The ELIP in SW China (Fig. 1a), which consists of massive flood basalts and numerous contemporaneous mafic and felsic intrusions, covers an area of more than $2.5*10^5$ km^2 with a total thickness ranging from several hundred meters up to 5 km (Xu et al., 2001; Xiao et al., 2003, 2004). In the eastern ELIP, the basalts unconformably overlie the Middle Permian Maokou Formation and are, in turn, overlain by the Xuanwei (terrestrial clastic rocks) and Longtan (marine clastic rocks) Formations, which are of the Lopingian (He et al., 2003, 2009). In the central part of the ELIP, the basalts overlie the Maokou Formation, and in turn are overlain by upper Triassic sedimentary rocks, indicative of deep erosion of the central ELIP.

Since the Early Permian a carbonate platform covered the South China Block (Wang et al., 1994; Feng et al., 1997; ECS, 2000).

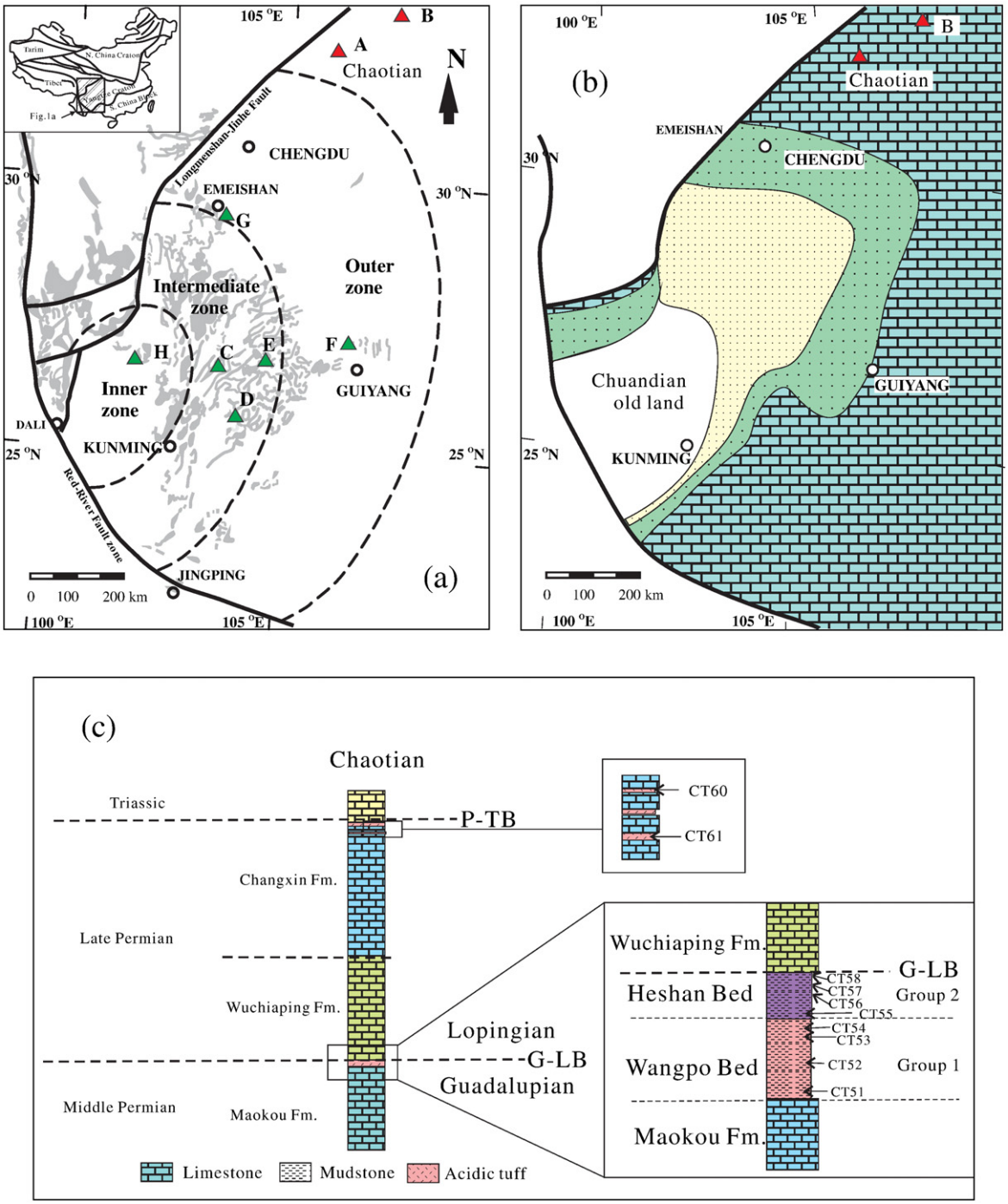

Fig. 1. (a) Schematic illustration of the geological features of the Emeishan large igneous province and the sampling locations. Dashed lines separate the inner, intermediate and outer zones, which are defined in terms of extent of erosion of the Maokou Formation (He et al., 2003); (b) lithofacies and paleogeography of the Late Permian (after the Emeishan volcanism) in the Upper Yangtze Craton (modified from He et al. (2006)); (c) stratigraphic sections and sampling localities at Chaotian. Triangle represents location of sampling section. Section A—Chaotian, Guangyuan city, northern Sichuan province; Section B—Liangshan, Shanxi province. Green triangles represent sampling locations of Xuanwei Formation by He et al. (2007), Zhou et al. (2000) and Huang (1997).

Emplacement of the ELIP in southwest China around the G–LB resulted in differentiation of this carbonate platform (He et al., 2006). The central ELIP, volcanism formed a subcircular uplift and lasted until the Late Triassic (Fig. 1b) (He et al., 2006). The areas outside of the ELIP are characterized by continuous carbonate platform sedimentation during the Permian except the G–LB marine regression (ECS, 2000). The marine regression at the Middle–Late Permian boundary (i.e., G–LB) resulted in deposition of a variable thick mudstone either at the basal part of the Wuchiaping Formation or between the Maokou and Wuchiaping Formations (Fig. 1c) (Wang et al., 1994; Feng et al., 1997; ESC, 2000). The distinct mudstone bed at the G–LB consists of two parts at the Chaotian section. The lower part is known as the Wangpo bed or G–LB "acidic tuff" and the upper part is known as the Heshan bed (Lai et al., 2008).

The Chaotian section is situated to the north of the ELIP (Fig. 1a), where the Permian carbonate platform was located (Fig. 1b). Recently, detailed studies on Permian biostratigraphic units at Chaotian have been conducted by Isozaki et al. (2004, 2007) and Lai et al. (2008). The G–LB and the end-Guadalupian mass extinction horizon were placed at the base of Wuchiaping Formation (Isozaki et al., 2007). The G–LB mudstones at the Chaotian section may record an erosional product of the ELIP. If correct, this section provides an opportunity to evaluate the temporal relationship between the extinction and the Emeishan volcanism.

With these aims in the mind, top to bottom sampling of the G–LB mudstones have been carried out at Chaotian (Fig. 1c). In addition, two samples of the Permian–Triassic Boundary (P–TB) acidic tuff at Chaotian have been sampled for the purpose of comparison.

3. Analytical methods

Identification of bulk and clay minerals were carried out on unoriented powder mounts by X-ray diffraction (XRD) (BRUKER D8 ADVANGE in German) at the Guangzhou Institute of Geochemistry, Chinese Academy of Sciences (GIGCAS). Qualitative and semi-quantitative characterization of mineralogy is based on peak intensity measurements on X-ray patterns. The diagnostic peak and the corrective intensity factor are indicated for each mineral. Semi-quantitative determination of the main clay species was based on the height of specific reflections, generally measured on ethylene glycol runs. The intensity of the 10 Å peak was taken as a reference, the other intensities were divided by a weight factor and all identified clay species values were summed up to 100%. Corrective factors were determined by long-term empirical experiments at GIGCAS.

All samples were analyzed for major element compositions at GIGCAS using wave-length X-ray fluorescence spectrometry (XRF). A pre-ignition was used to determine the loss on ignition (LOI) prior to major element analyses. Accuracy is within 1% for major elements. These samples were also selected for ICP-MS analysis of trace-element compositions. Accuracy for trace and rare earth elements is within 5%. Sample preparation techniques and other details are presented in Li et al. (2002).

4. Results

4.1. XRD results

Mineral compositions from XRD analyses are listed in Table 1. Representative XRD diagrams are shown in Fig. 2. Based on the mineralogy, mudstones at the Chaotian section are roughly divided into lower and upper parts, respectively corresponding to the Wangpo Bed and Heshan Bed (Table 1; Fig. 1c). The samples from the lower part (including sample CT51–54) are characterized by mixture of quartz (25.5–67.5%) and clay minerals. In particular, XRD data indicate that CT51 contains up to 67.5% quartz (Table 1; Fig. 2). In contrast, the samples from the upper part (including sample CT55–58) are characterized by mixture of clay minerals (mainly kaolinite, rectories and montmorillonite) and anatase (4.9–13%), with a subordinate amount of quartz (0.9–1.4%). Acidic tuffs at the Permian–Triassic boundary (CT60, 61) are dominated by illite (84.2–64.3%) with some quartz (5.2–8.8%) and feldspars (0–17.7%). Samples, CT52, 54, 55, 57 are abundant in calcite (20.1–43.8%). Especially CT-56 contains up to 43.8% calcite, indicating that the sample is a marlite or marl.

Table 1
Mineral compositions from XRD analyses of G–LB mudstones and acidic tuff at Chaotian.

Sample	Mineral compositions (wt.%)
CT-51	Rectories 17.7; feldspar 10.3; quartz 67.5
CT-52	Rectories 20.6; feldspar 11; quartz 48.3; calcite 20.1
CT-53	Rectories 33.6; montmorillonite 17.9; feldspar 9.5; quartz 25.5; calcite 11.9; anatase 1.6
CT-54	Illite 23.5; montmorillonite 22.6; quartz 29.8; calcite 20.9; anatase 3.2
CT-55	Montmorillonite 21; chamosite 18.4; quartz 1.4; calcite 43.9; anatase 5.8; goethite 9.5
CT-56	Kaolinite 20.6; halloysite 22.4; montmorillonite 10.3; quartz 1.7; calcite 40.1; anatase 4.9
CT-57	Kaolinite 42.9; rectories 8.7; saponite 34.2; quartz 1; calcite 1.3; anatase 10.5; hematite 1.3
CT-58	Kaolinite 40.4; rectories 42.5; feldspar 1.6; quartz 0.9; calcite 0.7; anatase 13.8
CT-60	Illite 64.3; feldspar 17.7; quartz 8.8; calcite 8.1; anatase 1.1
CT-61	Illite 82.2; quartz 5.2; calcite 10.5; hematite 2.1

4.2. Major elements

Major element compositions of the samples collected from G–LB mudstones and P–TB acidic tuff at the Chaotian section are listed in Table 1. Loss on ignition (LOI) ranges from 8% to 22% with most samples ~12%. High LOI contents are consistent with a high percentage of calcite and clay minerals in these rocks. The bulk rock analyses are characterized by high Al_2O_3 and Fe_2O_3 and low total alkali ($K_2O + Na_2O$) contents (0.4–2.11%), suggesting that these rocks were intensely weathered and altered. In particular, the samples collected from the upper part (CT57, 58) of the Chaotian section exhibit distinctively high content of Al_2O_3 (31.55%), Fe_2O_3 (2.33–5.6%) and TiO_2 (2.35–5.23%). For convenience, G–LB mudstones from Chaotian section are divided into two groups in terms of Al_2O_3/TiO_2 ratio, a ratio that remains virtually constant during surface weathering and alteration of rocks (Hayashi et al., 1997). Thus, this ratio is the most useful indicator for the provenance of sedimentary rocks (Taylor and McLennan, 1985; Hayashi et al., 1997) and acidic tuffs as well (Zhou and Kyte, 1988). Similar to the results from He et al. (2007), the Al_2O_3/TiO_2 ratios for the Group 1 sediments are greater than 7 whereas the ratios for the Group 2 sediments are less than 7.

Group 1 sediments from the Chaotian section are characterized by high Al_2O_3/TiO_2 (13.6–39.6), which is very similar to the ratio (11–43) of the rhyolites and tuffs in the upper sequence of the lava succession at Binchuan (Zhang et al., 1988; Xu et al., 2010). The highest Al_2O_3/TiO_2 ratio (39.9) is noted for sample CT51, a value typical of felsic extrusives (Hayashi et al., 1997). Group 2 sediments including CT55, 57, 58 occupy the upper part of G–LB mudstones and show significantly lower Al_2O_3/TiO_2 ratios (5.94–6.35) except CT-53(9.54). This range in Al_2O_3/TiO_2 ratio is comparable with those of the Emeishan basalts in the center of the province (Xu et al., 2001).

4.3. Trace elements

The Group 1 and Group 2 sediments are also distinct in terms of the minor and trace-element compositions. Total rare earth element (REE) contents (148–524 ppm) in Group 1 samples are higher than Group 2 mudstones (118–186 ppm; Table 2, Fig. 3), however, contents of high

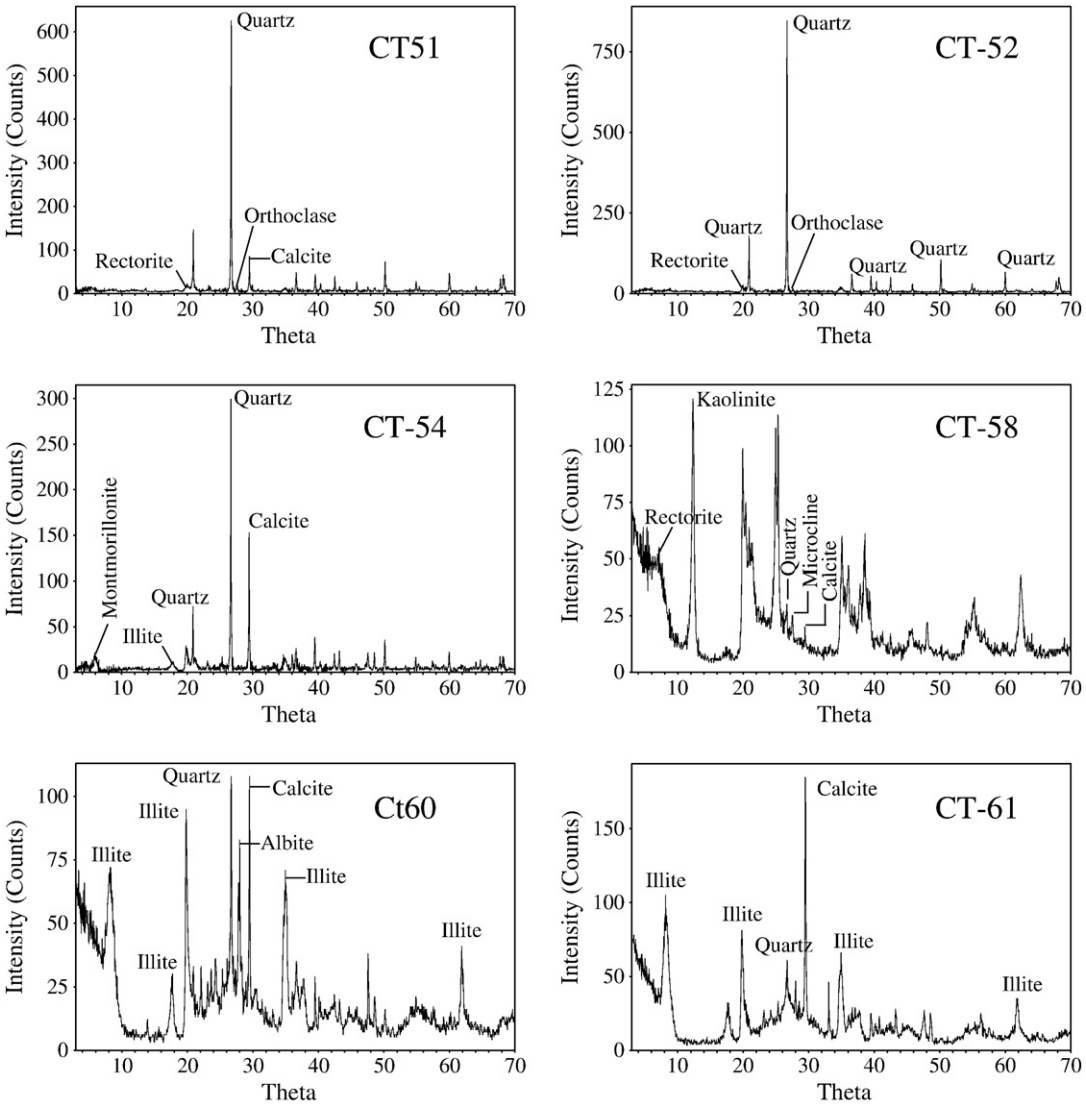

Fig. 2. Representative XRD patterns of G–LB mudstones and acidic tuffs at Chaotian section.

field strength elements (HFSE) in Group 2 samples (525–1320 ppm) are much higher than those in Group 1 samples (181–426 ppm; Table 2). REE patterns of Group 1 and Group 2 are similar, both have weakly fractionated and possess moderately negative Eu anomalies (0.64–0.74, Fig. 3), resembling REE pattern of upper continent crust (Taylor and McLennan, 1985).

5. Discussions

5.1. Are G–LB mudstones at Chaotian acidic tuff?

As mentioned above, G–LB mudstones at Chaotian section are divided into two layers. The lower layer is called the "G–L boundary acidic tuff" or Wangpo Bed (Isozaki et al., 2004; Isozaki and Ota, 2007). The upper layer is called the Shale Bed (Isozaki and Ota, 2007) or Heshan Bed (Lai et al., 2008). Isozaki et al. (2004), based on XRD, XRF and SEM analyses, suggested that the Wangpo Bed is composed mainly of mixture of illite–montmorillonite with euhedral apatites, zircons, and bipyramidal quartz (Isozaki et al., 2004). This led them to conclude that this clay bed originated from a volcanic ash of rhyolitic to dacitic composition, and must have covered most of South China at the G–LB or end-Guadalupian (Isozaki et al., 2004; Isozaki and Ota, 2007).

To examine this hypothesis, we analyzed 4 samples from the Wangpo Bed and 4 samples from Heshan Bed at Chaotian section. XRD analyses show that four samples from Wangpo Bed are characterized by high quartz content (25.5–68%), with a maximum of 67.5% quartz in the sample CT51 (Table 1; Fig. 2). Since air-fall acidic tuff generally contains 1–10% quartz (Altaner and Grim, 1990; Zhou, 1999), a high content of quartz grains (up to 68%) indicates that the Wangpo bed is not an acidic tuff, but likely represents fine clastic sedimentary rocks. Some euhedral minerals such as apatite, zircon, plagioclase, and bipyramidal quartz have been used as identification criteria for acidic tuffs (Isozaki et al., 2004), but caution should be applied with this approach, because euhedral minerals may be also derived from the redeposition of felsic volcanic rocks. In addition, while selecting zircons from the Wangpo Bed, it is apparent that most zircons are rounded although a few euhedral zircons are also found. This is inconsistent with the origin of acidic tuffs.

The Al_2O_3/TiO_2 ratio is one of the most useful indicators of acidic tuffs or tonsteins (Spears and Kanaris-Sotiriou, 1979; Zhou et al., 1982; Zhou and Kyte, 1988). Zhou and Kyte (1988) documented that Al_2O_3/TiO_2 ratio of acidic tuff at the Permian–Triassic Boundary is about 80. Zhou (1999) also complied 295 samples of tonsteins and mudstones from the Upper Permian in this region and concluded that the Al_2O_3/TiO_2 weight ratio of the acidic tuffs range from 28.8 to 310.7

Table 2
Major and trace elements of G–LB mudstones and acidic tuffs at Chaotian.

	CT51	CT52	CT53	CT54	CT57	CT55	CT56	CT58	CT60	CT61
	Group 1					Group 2		Acidic tuff		
Al_2O_3	14.54	15.02	14.39	14.93	30.69	14.59	16.68	31.55	25.13	24.05
CaO	5.19	0.71	4.91	8.99	1.37	23.80	21.36	0.97	4.26	6.31
Fe_2O_3	4.34	5.16	5.11	9.18	5.60	10.20	8.84	2.36	2.49	2.56
K_2O	1.55	1.70	1.92	1.40	0.63	0.57	0.33	0.55	4.13	4.67
MgO	0.83	0.76	1.37	1.05	0.73	0.43	0.38	0.71	1.59	2.31
MnO	0.12	0.08	0.01	0.00	0.00	0.01	0.01	0.00	0.01	0.02
Na_2O	0.27	0.15	0.18	0.14	0.11	0.12	0.11	0.11	1.12	0.28
P_2O_5	0.62	0.20	0.03	0.04	0.03	0.03	0.04	0.03	0.40	0.18
SiO_2	60.10	68.47	60.52	48.55	43.48	22.02	23.92	44.57	50.10	46.14
TiO_2	0.37	0.39	0.88	1.10	3.22	2.19	2.44	5.31	0.45	0.44
L.O.I	11.97	7.45	10.31	14.27	14.05	26.03	25.60	13.80	10.19	12.57
Total	99.89	100.07	99.63	99.64	99.92	99.99	99.70	99.96	99.87	99.53
CIA	0.85	0.86	0.84	0.88	0.97	0.93	0.96	0.97	0.75	0.80
Al_2O_3/TiO_2	39.63	38.88	16.33	13.62	9.52	6.67	6.85	5.94	55.94	54.39
Sc	12.73	13.76	18.63	11.10	18.54	16.15	16.64	31.48	3.38	12.32
V	720.50	780.40	3968.20	3776.40	2836.70	4046.40	2941.60	1951.30	65.45	51.04
Cr	2805.70	1995.50	2051.70	1937.80	563.90	1253.10	1110.30	500.60	16.43	10.86
Mn	953.60	562.50	77.81	29.67	9.54	15.14	55.37	5.83	84.40	134.90
Co	42.27	59.79	15.67	9.25	9.41	6.76	10.52	4.96	10.99	16.80
Ni	821.60	605.50	36.22	38.62	344.70	97.40	166.10	268.90	27.54	34.58
Cu	147.40	213.50	78.64	60.35	272.70	56.19	101.00	224.90	44.61	93.89
Zn	773.20	516.30	4.37	8.18	87.73	35.73	29.52	88.10	68.26	71.99
Ga	12.28	11.07	33.78	30.17	33.06	21.49	24.84	44.07	23.25	26.97
Ge	2.76	2.44	1.53	1.85	1.53	1.62	2.03	0.61	0.64	1.11
Rb	70.24	56.38	67.83	57.55	17.97	22.16	12.70	13.04	128.10	157.50
Sr	222.40	292.90	72.53	112.00	47.19	90.93	86.17	45.69	972.20	644.50
Y	295.60	75.94	28.02	33.04	30.67	31.73	33.94	40.85	25.22	63.85
Zr	117.40	93.63	220.30	299.30	712.70	430.70	502.60	1120.20	287.10	484.30
Nb	8.58	8.15	20.15	26.93	73.77	48.48	54.94	124.30	10.58	10.76
Cs	3.00	3.99	9.91	7.78	2.52	2.86	2.34	2.29	7.98	10.02
Ba	274.10	348.80	178.40	171.80	50.56	61.11	54.45	45.29	76.05	54.20
La	128.10	57.72	39.12	57.54	29.08	48.20	46.40	22.85	77.47	102.30
Ce	231.60	141.80	69.82	91.35	59.66	88.65	77.08	51.21	157.30	210.90
Pr	26.49	18.27	8.29	8.70	7.63	10.06	9.07	7.32	18.85	25.78
Nd	113.90	74.72	25.84	23.31	27.33	32.97	28.24	27.45	62.10	86.08
Sm	19.47	13.86	4.15	2.93	6.00	5.08	4.95	7.21	10.78	16.22
Eu	4.56	3.17	0.89	0.67	1.37	1.18	1.14	1.64	1.43	1.93
Gd	24.67	11.90	3.48	2.77	5.65	5.03	5.02	7.50	7.57	14.26
Tb	3.76	1.90	0.73	0.66	1.07	0.99	1.03	1.49	1.14	2.26
Dy	22.07	10.25	4.87	4.93	6.13	6.09	6.21	8.33	6.02	12.14
Ho	4.96	2.12	1.05	1.13	1.18	1.21	1.28	1.59	1.12	2.39
Er	13.62	5.48	2.94	3.40	3.07	3.16	3.24	4.17	2.85	6.14
Tm	1.83	0.80	0.52	0.57	0.48	0.49	0.52	0.67	0.44	0.87
Yb	10.49	5.15	3.51	4.04	3.19	3.10	3.41	4.57	2.76	5.26
Lu	1.68	0.82	0.55	0.61	0.51	0.47	0.52	0.70	0.38	0.77
Hf	3.19	2.38	5.10	7.19	16.93	10.37	12.44	25.15	8.52	13.68
Ta	0.75	0.66	1.66	2.19	5.70	3.63	4.28	9.08	2.15	2.75
Pb	23.91	16.41	22.99	37.45	40.28	19.29	27.85	26.93	35.11	42.49
Th	8.14	7.18	10.92	7.42	21.31	13.05	17.24	34.34	45.94	60.07
U	25.72	11.20	23.13	28.22	52.75	45.88	43.38	79.41	9.02	12.68
Eu/Eu*	0.64	0.74	0.70	0.70	0.71	0.71	0.69	0.68	0.46	0.38
REE	607.21	347.97	165.75	202.60	152.34	206.69	188.10	146.69	350.20	487.30

$Eu/Eu^* = Eu_N/(Sm_N + Gd_N)^{1/2}$. *N*: normalized, normalization value after Taylor and McLennan (1985); REE means Total Rare Earth Elements.

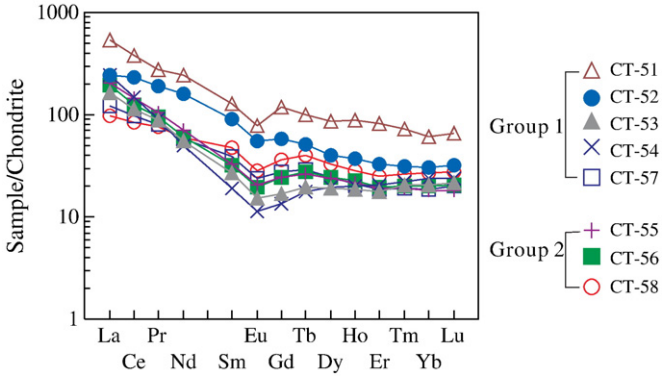

Fig. 3. Chondrite-normalized REE patterns of G–LB mudstones and acidic tuffs at Chaotian section. Normalization values are from Sun and McDonough (1989).

with an average of 85.7. In the case of the Wangpo bed, the Al_2O_3/TiO_2 ratios of the two samples (i.e. CT53, 54) are 16.3 and 13.6 respectively, which are much lower than average ratio of acidic tuffs in this region. In addition, the content of Fe_2O_3 (4.34–9.18%) in the Wangpo Bed is also significantly higher than one of the acidic tuff (0.74–2.45) (Kramer et al., 2001).

Acidic tuffs commonly have strong negative Eu anomaly (Kramer et al., 2001). The Eu/Eu* of P–TB tuff ranges from 0.23 to 0.47 (Zhou and Kyte, 1988). The two P–TB tuffs we analyzed have Eu/Eu* values of 0.38 and 0.46, thus consistent with previous studies. The Eu/Eu* values of Wangpo Bed range from 0.64 to 0.74 (Table 2), much higher than those of typical acidic tuff. Immobile trace elements (e.g. Zr, Nb, Y and Ti) are commonly used to constrain the origin of volcanic ashes or tuffs (Kramer et al., 2001). In TiO_2/Zr versus Nb/Y diagram (Kramer et al., 2001), CT51 and CT52 fall within the andesite field and CT53, 54

fall within the trachyandesite field (Fig. 4). In other words, Group 1 samples are not likely to be rhyolites or dacites and therefore the results are inconsistent with the origin of acidic tuffs. Moreover, four samples of the Wangpo Bed vary greatly in their mineralogy and geochemistry. Considering all of the available evidence, it seems that the Wangpo Bed is not an acidic tuff. Integration of mineralogical and geochemical analyses of the Wangpo Bed suggests that the G–LB mudstones or Wangpo Bed are not air-fall acidic tuffs despite the presence of euhedral apatite and zircon. Instead they likely represent detrital or clastic sedimentary rocks. The proposition that the G–LB acidic tuff bed covers an area of 2000 km × 1500 km in South China (Isozaki et al., 2004; Isozaki and Ota, 2007; Isozaki, 2007) also remains questionable. For instance, G–LB mudstones at Liangshan, Shanxi province and at Yunxin, Guizhou province show similar compositional characteristics as the Chaotian mudstones, therefore it cannot be an acidic tuff (He, unpublished data). As a consequence, the volcanic ash origin of the Wangpo Bed in SW China, as proposed by Isozaki et al. (2007), should be reconsidered.

5.2. Provenance of mudstones at the Choatian section

Factors controlling the geochemistry of a clastic sedimentary rock include: (1) composition of source terrain, (2) chemical weathering, (3) hydraulic sorting, (4) diagenesis, (5) metamorphism, and (6) hydrothermal alteration. Since the G–LB mudstones from the Chaotian section were not metamorphosed or altered, diagenetic influences are likely minor. Below, we concentrate our discussion on the first three factors.

5.2.1. Paleogeography at G–LB and possible sources for the Chaotian mudstones

As mentioned previously, the subcircular uplift, called the Chuandian "old land" in Chinese geologic literature (Wang et al., 1994; Feng et al., 1997), existed in the inner zone of the ELIP after the main period of Emeishan volcanism (Fig. 1b) and was maintained until the late Triassic (He et al., 2006). It is interesting to note that the distribution of the Xuanwei Formation and Longtan Formation is exclusively around this "old land" (Fig. 1b). Such a spatial configuration and paleogeography is strongly indicative of a genetic linkage between the uplift (and erosion) of the old land and the formation (and deposition) of the clastic rocks. Due to the existence of the Qinling sea trench in the north and Songpan basin in the west, the Chuandian "old land" is the only possible source for G–LB mudstones at Chaotian. In other words, the central ELIP is only possible source for the Xuanwei and Longtan Formations, and G–LB mudstones in SW China.

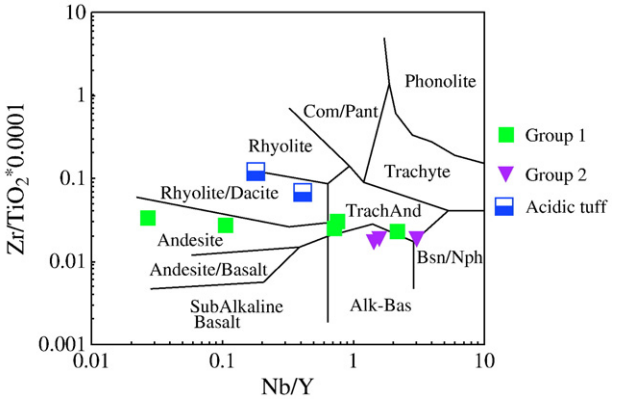

Fig. 4. TiO_2/Zr versus Nb/Y diagram of G–LB mudstones and acidic tuffs at Chaotian section. Lines dividing mafic, intermediate and felsic are modified from Hayashi et al. (1997). Mafic and felsic area of the Emeishan LIP from Zhang et al. (1988) and Xu et al. (2001).

5.2.2. Chemical weathering

The most widely used chemical index to ascertain the degree of source-area weathering is the Chemical Index of Alteration (CIA). This index is calculated using molecular proportions as shown in the equation below: $CIA = Al_2O_3/(Al_2O_3 + CaO + Na_2O + K_2O)$. In the equation, CaO^* is the amount of CaO incorporated in the silicate fraction of the rock. Correction for CaO from carbonate contribution was not done for the clayey rocks since there was no CO_2 data. Therefore, to compute the CaO^* from the silicate fraction, the method of Bock et al. (1998) was used. In this regard, CaO values were accepted only if $CaO \leq Na_2O$. Consequently, when $CaO > Na_2O$, it was assumed that the concentration of CaO equals that of Na_2O (Bock et al., 1998). The calculated CIA values for the mudstones from the Chaotian section (Table 2) range between 84 and 97 with a mean of 92, indicating extreme weathering. In comparison the CIA values of two samples from the Permian–Triassic acidic tuffs are 75 and 80, corresponding to moderate weathering.

5.2.3. Provenance of G–LB mudstones at Chaotian section

Since there are only two possible sources (mafic and felsic parts of the ELIP) for the Chaotian G–LB mudstones we compare them with the ELIP. XRD analyses show that four samples from the Wangpo Bed are characterized by a high content of quartz (25.5–68%), with a maximum of 68% quartz. Because basalts generally contain little quartz, high quartz abundances indicate that the source of the mudstones may have been derived from felsic extrusives. On the other hand, four samples (i.e., CT55–58) from Heshan Bed are characterized by a mixture of clay minerals (mainly kaolinite, rectories and montmorillonite) and anatase (4.9–13.8%). High abundances of anatase (up to 13.8%) and little quartz indicate that their source may be linked to mafic igneous rocks.

5.2.3.1. Major elements. The Al_2O_3/TiO_2 ratio is the most useful provenance indicator of sedimentary rocks for two reasons (Hayashi et al., 1997). Firstly, in igneous rocks, Al resides mostly in feldspars and Ti resides within mafic minerals (e.g., olivine, pyroxene, hornblende, biotite, ilmenite lots in accessory minerals). Therefore, the A1/Ti ratio of igneous rocks generally increases with increasing SiO_2 content; the data compiled by Hayashi et al. (1997) shows that the Al_2O_3/TiO_2 weight ratio increases from 3 to 8 for mafic igneous rocks (SiO_2 = 45–52 wt.%), 8–21 for intermediate igneous rocks (SiO_2 = 53–66 wt.%), and 21–70 for felsic igneous rocks (SiO_2 = 66–76 wt.%) (Hayashi et al., 1997). In the central ELIP, for example, the Al_2O_3/TiO_2 ratio of basalts ranges from 3 to 5.91 with an average of 4.11 (Zhang et al., 1988; Xu et al., 2001), whereas for felsic rocks the ratio ranges from 11.4 to 42.7 with an average of 24.7 (Xu et al., 2010). Secondly, it is widely accepted that the Al_2O_3/TiO_2 ratios of most clastic sedimentary rocks are essentially identical to those of their source rocks (Sawyer, 1986; Nesbitt and Wilson, 1992; Maynard, 1992; Mai, 1993; Hayashi et al., 1997). Hayashi et al. (1997) showed that Al_2O_3/TiO_2 in mudstones and sandstones is similar to that of the parent rocks. In most cases, the fractionation of A1 and Ti is insignificant between silts/shales and their parent rocks, probably because most Ti in weathered rocks occurs as a chemical constituent of chlorite (and other clays) and/or as minute ilmenite inclusions in these silicate minerals, rather than as separate ilmenite grains (Hayashi et al., 1997 and references therein). Therefore, the Al_2O_3/TiO_2 ratio is used as an indicator of source rocks, especially of igneous rocks.

The Al_2O_3/TiO_2 ratio of the Wangpo bed at Chaotian section ranges between 12 and 40 (Table 2), indicating that the 4 mudstone samples (i.e., CT51–54) of Wangpo Bed and CT57 belong to Group 1. Specifically, Al_2O_3/TiO_2 of sample CT51, 52 is as high as 38–40, a value typical of felsic volcanics (Hayashi et al., 1997). This ratio is also similar to that of the felsic extrusives in the upper ELIP at Binchuan (Xu et al., 2010). The Al_2O_3/TiO_2 ratio of sample CT53 and CT-4 are

13.6, 16.4, respectively, which are much lower than P–TB acidic tuff samples (sample CT60, 61) at Chaotian. On the other hand, Al_2O_3/TiO_2 of the Heshan Bed (Group 2 except CT-57) is significantly lower, ranging from 5.95 to 6.85 with an average of 6.35 (Table 1). This value is slightly higher than that of the Emeishan basalts (3.9–5.9) in the center of the province. This suggests a possible input from mafic sources. Bivariate plots of TiO_2 (%) and Al_2O_3 (%) are also used extensively for determining source rock compositions (McLennan et al., 1980; Schieber, 1992). From Fig. 5, it is clear that the Wangpo Bed plots near the felsic field, whereas Heshan Bed is mostly confined to a mafic compositional field.

5.2.3.2. Trace elements. Trace-element abundances and ratios of some immobile elements in the clastic rocks further assist with provenance analyses. REE compositions can also be used for monitoring the source composition because mafic rocks generally show less fractionated REE patterns with low LREE/HREE ratios and weak to no Eu anomalies (Cullers and Graf, 1984). In contrast, felsic rocks usually show fractionated chondrite-normalized patterns and strong negative Eu anomalies. Such characteristics may be preserved in sedimentary rocks (McLennan et al., 1980; Cullers and Podkovyrov, 2002; Lopez et al., 2005).

The REE abundance in the Group 1 sediments is higher than in the Group 2 samples (Table 2, Fig. 3). Group 2 sediments show less fractionated REE patterns with low LREE/HREE ratios and weak Eu anomalies compared to Group 1 samples. However, both of the Group 1 and Group 2 samples possess moderate negative Eu anomalies. This indicates that although Group 1 and Group 2 may be derived from felsic and mafic igneous rocks, respectively, some mixing of source sediments may have occurred. For example average Al_2O_3/TiO_2 ratio of Group 2 is 6.35, which is slightly higher than the average Al_2O_3/TiO_2 ratio of basalts (4.3), implying some input from a felsic source. REE patterns of Group 1 differ from acidic tuffs in LREE/HREE ratio and Eu anomalies (Fig. 3), but resemble alkaline granites in the central ELIP (Zhang et al., 1988). In the TiO_2/Zr versus Nb/Y diagram, Group 1 falls within the andesite and trachyandesite fields, whereas Heshan Bed or Group 2 falls towards the margins of the basalt field (Fig. 4). This also implies that minor mixing between the sources of Group 1 and Group 2 sediments. In the TiO_2 versus Zr diagram, Group 1 and Group 2 samples respectively fall in the margins of felsic and basalt fields (Fig. 6), implying their likely sources and minor mixing.

In summary, mineralogical and geochemical analysis of G–LB mudstones at Chaotian suggests that Wangpo Bed was derived from felsic part of the Emeishan LIP, though some samples may have mixed source compositions, whereas Heshan bed was mainly derived from mafic lavas of the ELIP. Decoupling between major and trace elements may be caused by extreme weathering and hydraulic sorting.

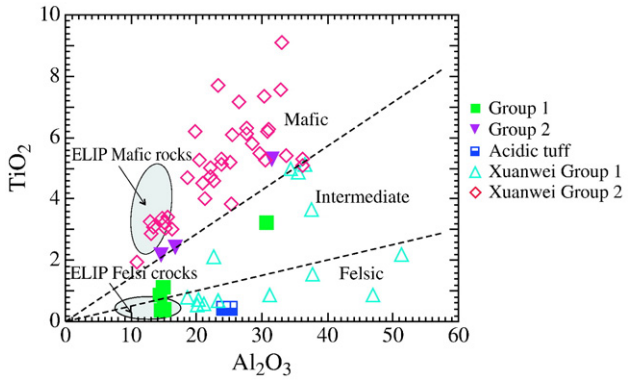

Fig. 5. Bivariate plots of TiO_2 (%) and Al_2O_3 (%) of G–LB mudstones and acidic tuffs at Chaotian section. Data of the Xuanwei Formation are from He et al. (2007).

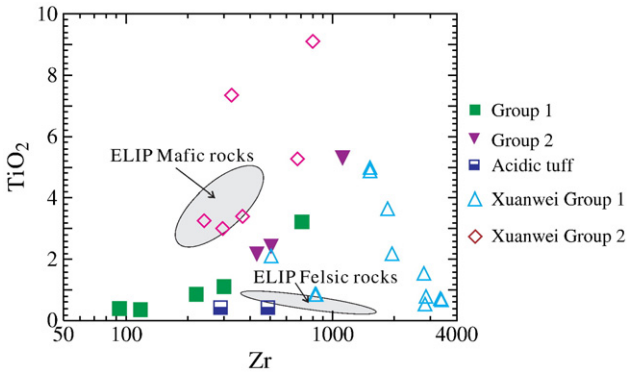

Fig. 6. TiO_2 versus Zr diagram of G–LB mudstones and acidic tuffs at Chaotian section. Mafic and felsic area of the Emeishan LIP from Zhang et al. (1988) and Xu et al. (2001). Data of the Xuanwei Formation are from He et al. (2007).

5.3. Temporal coincidence between end-Guadalupian mass extinction and the Emeishan flood volcanism

Previous studies of three sections of the Xuanwei Formation east of the ELIP showed that the lowermost part (Group 1) of Xuanwei Formation represents eroded materials of the felsic member of the uppermost sequence of the Emeishan volcanic succession; whereas the other part (Group 2) is compositionally more akin to the mafic rocks (Fig. 7a; He et al., 2007). This conclusion was also supported by other studies. Zhang et al. (1988) pointed out that acidic volcanic flows developed in lowermost of Xuanwei Formation. Zhou (1999) and Zhou et al. (2000) studied 8 sections of Xuanwei Formation in the east of the Emeishan LIP and concluded that alkaline acidic volcanic tuff layer was generally developed in the lower part of Xuanwei Formation (e.g., section F in Fig. 7b). Huang (1997) reported a REE deposit within the Xuanwei Formation on the top of the Emeishan basalts (section E in Figs. 7b and 1). Based on strong fractioned REE pattern and strong negative Eu anomaly, he suggested that this deposit may be derived from felsic members of the Emeishan succession. Thus, Group 1 sediments in the lowermost part of Xuanwei Formation may be a common feature in the region.

As discussed above, G–LB mudstones at Chaotian are also derived from the erosion of the ELIP. The lower part of the Wangpo Bed (Group 1) is chemically similar to the felsic rocks whereas the upper part of the Heshan Bed (Group 2) is chemically similar to the mafic rocks. This chemo-stratigraphy is identical to that observed for the Xuanwei Formation (He et al., 2007). This layer of mudstone was also called Longtan Formation in Chinese geological community (ESC, 2000). Thus, G–LB mudstones are well correlated with Xuanwei Formation and Longtan Formation (Fig. 7a). Taking into account the rapid regression that occurred at the G–LB, the Chaotian G–LB mudstones may be equivalent to Longtan and Xuanwei Formations.

Moreover, the ELIP does have felsic extrusive in the uppermost unit of lava sequence (Zhang et al., 1988; Xu et al., 2001, 2010; Ali and Wignall, 2007; Shellnutt and Jahn, 2010), a feature shared by other continental LIPs such as the Etendeka, Karoo and Yemen (Bryan et al., 2002). It is documented that at least four sections have variably thick felsic extrusives (i.e., rhyolite, trachyte) of the upper part of the Emeishan LIP in the inner zone (Zhang et al., 1988). But, due to deep erosion in the central ELIP, most of these felsic rocks may have been eroded away and deposited in an eastern Late Permian basin. Ali and Wignall (2007) also reached a similar conclusion on the basis of Chinese geological reports (Zhang et al., 1988; BGMRSP, 1991) that acidic rocks in the Emeishan basalt sections, particularly in the waning interval rocks, can be assigned to the Xuanwei Formation.

Given the fact that the spatial distribution of the Xuanwei Formation occurs exclusively surrounding the Chuandian old land (Fig. 1b), it is likely that the Group 1 sediments in the lowermost Xuanwei Formation

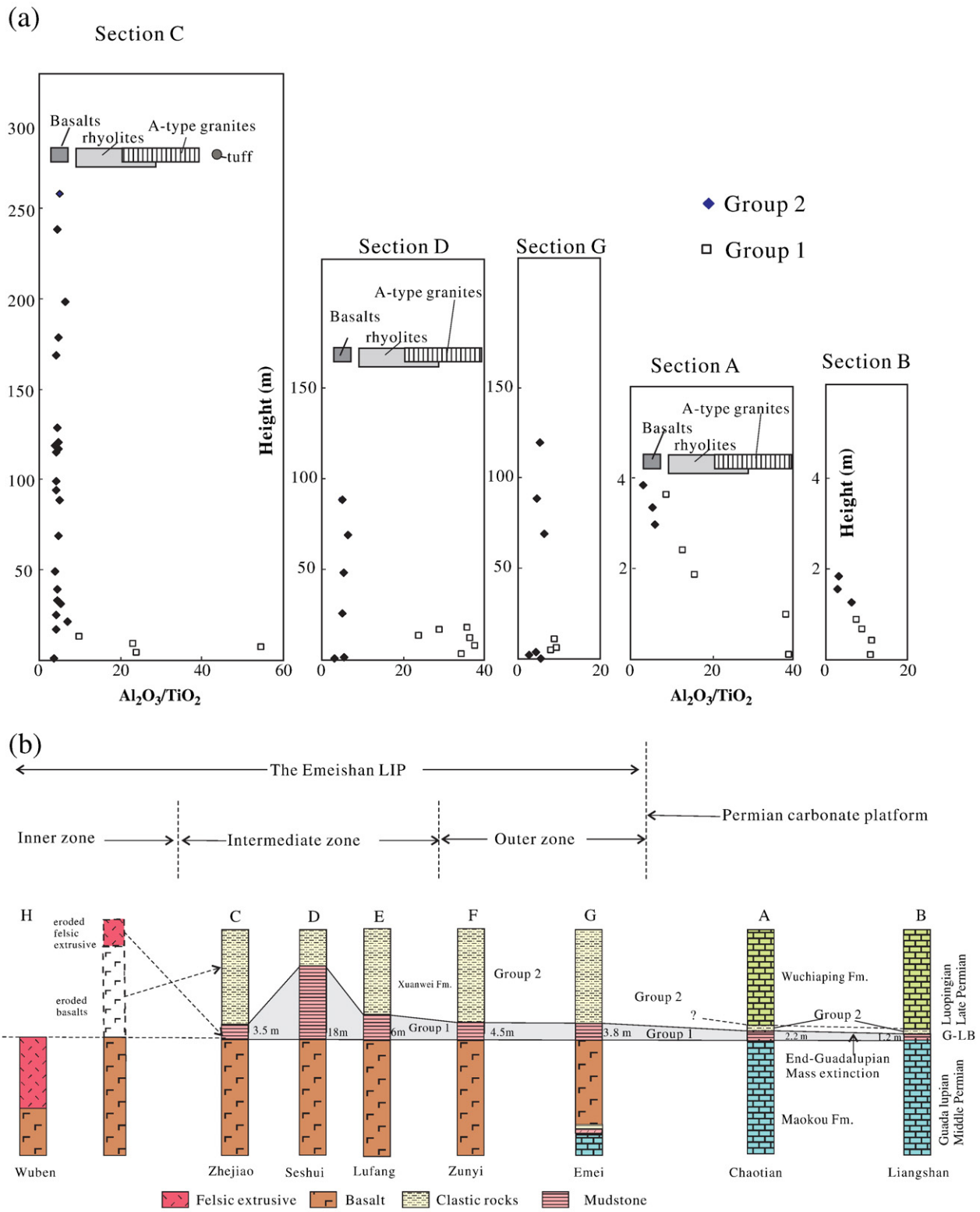

Fig. 7. (a) Plot of Al_2O_3/TiO_2 ratio for the mudstones against their stratigraphic height at Chaotian section and its correlation with the Xuanwei Formation. Locations of sections are shown in Fig. 1. See text for the definition of Group 1 and Group 2 sediments. The ranges of Al_2O_3/TiO_2 ratio for the Emeishan basalts and A-granites are from Zhang et al. (1988) and Xu et al. (2001). The rhyolites and tuff were sampled from the center of the Emeishan large igneous province (Xu et al., in press). (b) Chemostratigraphic correlation in the Emeishan LIP and South China suggesting the emplacement of the Emeishan flood volcanism at the Middle–Late Permian boundary. Geochemically, Group 1 and Group 2 sediments of the Xuanwei Formation are related to the felsic and mafic components of the central Emeishan LIP, respectively. The stratigraphic sequence that the felsic-derived Group 1 and the mafic-derived Group 2 sediments is the reverse of the volcano-stratigraphy of the Emeishan volcanism where felsic extrusives postdated mafic extrusives. It is likely that the Xuanwei sediments resulted from unroofing, erosion and deposition of Emeishan volcanic rocks from the central LIP. Keys are the same as in Fig. 1.

were derived from the felsic members of the Emeishan LIP, and the Group 2 sediments from the mafic rocks (Fig. 7b). In support of this interpretation, the stratigraphic sequence of mafic-related Group 2 samples overlie the felsic-related Group 1 rocks in the Permian of SW China is the reverse (as expected during erosional unroofing) of the volcanic sequence of the Emeishan lavas in which the rhyolites and

trachytes occur above the basaltic lavas (Fig. 7). The uppermost silicic members in the center of the LIP were eroded first and the "felsic" materials were transported and deposited in the eastern LIP, forming the lowermost part of the Xuanwei Formation. Further erosion uncovered the mafic part of the Emeishan LIP and this eroded "mafic" material was deposited over those sediments derived from the felsic flows (Fig. 7). This interpretation is also supported by the general agreement between the age of the lowermost Xuanwei Formation (257 ± 4 Ma; 260 ± 4 Ma) and that of the silicic ignimbrite in the uppermost of the Emeishan lava succession (263 ± 5 Ma). Hf isotopic compositions of zircons from Group 1 sediments, G–LB mudstones and Emeishan acidic rocks are essentially the same (ε_{Hf} = 3.5 and 12.6; He et al., unpublished; Xu et al., 2008; Shellnutt et al., 2009). Therefore, G–LB mudstones at Chaotian section are well correlated with the lowermost part (Group 1) of the Xuanwei Formation and the uppermost felsic part (may be eroded) of the Emeishan succession in the central ELIP (Fig. 7).

The genetic linkage of the Wangpo Bed at Chaotian section and lowermost part (Group 1) of Xuanwei Formation with the latest Emeishan silicic rocks yields an important implication regarding the relative timing between the Guadalupian mass extinction and Emeishan volcanism. Given the fact that the Wangpo Bed is likewise genetically related to Emeishan silicic volcanism, it follows that the felsic member in the uppermost Emeishan basalts, Group 1 sediments of Xuanwei Formation and Wangpo Bed at the Late–Middle Permian boundary all lie on an isochron horizon (Fig. 7b). This correlation and erosional provenance of the G–LB mudstones suggest that the Emeishan flood volcanism was terminated before the Middle–Late Permian boundary or G–LB (Fig. 7b). This direct evidence thereby provides a new constraint on the temporal coincidence between Emeishan flood volcanism and the end-Guadalupian biotic crisis. In addition, since both the Emeishan basalts and the Chaotian G–LB mudstones rest on the Maokou Formation, the Emeishan basalts are therefore roughly inferred to be the stratigraphic equivalent of the Wangpo Bed at the Chaotian section, indicating a short eruption period. The relative temporal coincidence of these two phenomena and rapid eruption of the ELIP may support the idea of a cause-and-effect relationship.

6. Conclusions

Based on mineralogical and geochemical analyses of G–LB mudstones from Chaotian section, the following conclusions can be drawn:

(1) The G–LB mudstones at Chaotian represent clastic rocks derived from the ELIP, rather than acidic tuff as proposed by Isozaki et al. (2004). Previous interpretations of G–LB layers in SW China as acidic tuffs are in need of further investigation. The Wangpo Bed at Chaotian section may be mainly from felsic volcanic rocks, while the Heshan Bed was mainly derived from mafic lavas. Such a chemostratigraphic sequence is the same as that for the Xuanwei Formation (He et al., 2007).

(2) Correlation of G–LB mudstones at Chaotian with Xuanwei and Longtan Formations and the Emeishan felsic extrusives indicates the termination of the Emeishan volcanism *before* the G–LB and a relative temporal coincidence between the ELIP and the end-Guadalupian mass extinction. The data presented in this study thus support the idea of a cause-and-effect relationship between two phenomena.

Acknowledgements

This research was supported by grants from the National Natural Science Foundation of China (40721063), National Basic Research Program of China (973 Program) (2007CB411401) and the CAS/SAFEA International Partnership Program for Creative Research Teams. The author would like to thank the constructive reviews by Michael Brookfield, Greg Shellnutt and an anonymous referee. The paper also benefited from discussions with Dr. Sun Weidong and Dr. Wei Gangjian, and language correction by Scott Paterson. This is contribution No IS-XXX from GIGCAS.

References

Ali, J.R., Thompson, G.M., Zhou, M.F., Song, X.Y., 2005. Emeishan large igneous province, SW china. Lithos 79, 475–489.
Ali, J.R., Wignall, P.B., 2007. Comment on "Fusiline biotic turnover across the Guadaluplan–Lopingian (middle–upper Permian) boundary in mid-oceanic carbonate build-ups: biostratigraphy of accreted limestone in Japan" by Ayano Ota and Yukio Isozaki. Journal of Asian Earth Science 30, 199–200.
Altaner, S.P., Grim, R.E., 1990. Mineralogy, chemistry and diagenesis of tuffs in the Suker Creek Formation (Miocene), eastern Oregon. Clays and Clay Minerals 38, 561–572.
Bock, B., Mclennan, S.M., Hanson, G.N., 1998. Geochemistry and provenance of the Middle Ordovician Austin Glen Member (Normanskill Formation) and the Taconian Orogeny in New England. Sedimentology 45, 635–655.
Bryan, S.E., Rilly, T.R., Jerram, D.A., Stephens, C.J., Leat, P.T., 2002. Silicic volcanism: an undervalued component of large igneous provinces and volcanic rifted margins. In: Menzies, M.A., Klemperer, S.L., Ebinger, C.J., Baker, J. (Eds.), Volcanic Rifted Margins: Boulder, Colorado: Geological Society of American Special Paper, vol. 362, pp. 99–120.
Bureau of geology and mineral resources of Sichuan province (BGMRSP), 1991. Regional Geology of Sichuan Province. Geological Publishing House, Beijing. 745 pp. (in Chinese with English abstract).
Courtillot, V., Jaupart, C., Manighetti, I., Tapponnier, P., Besse, J., 1999. On causal links between flood basalts and continental breakup. Earth And Planetary Science Letters 166, 177–195.
Cullers, R.L., Graf, J.L., 1984. Rare earth elements in igneous rocks of the continental crust: intermediate and silicic rocks-ore petrogenesis. In: Henderson, P. (Ed.), Rare-Earth Geochemistry. Elsevier, Amsterdam, pp. 275–312.
Cullers, R.L., Podkovyrov, V.N., 2002. The source and origin of terrigenous sedimentary rocks in the Mesoproterozoic Ui group, southeastern Russia. Precambrian Research 117, 157–183.
Editing Committee of Stratigraphy (ECS), 2000. Permian in China. Geological Publishing House, Beijing. 149 pp. (Chinese with English abstract).
Fan, W.M., Wang, Y.J., Peng, T.P., Miao, L.C., Guo, F., 2004. Ar–Ar and U–Pb chronology of late Palaozoic basalts in western Guangxi and its constraints on the eruption age of the Emeishan basalt magmatism. Chinese Science Bulletin 49, 2318–2327.
Feng, Z.Z., Yang, Y.Q., Zin, Z.K., 1997. Lithofacies Paleogeography of Permian of South China. Petroleum Univ. Press, Beijing. (in Chinese with English abstract).
Guo, F., Fan, W.M., Wang, Y.J., Li, C.W., 2004. When did the Emeishan mantle plume activity start? Geochronological and geochemical evidence from ultramafic–mafic dikes in southwestern China. International Geology Review 46, 226–234.
Hallam, A., Wignall, P.B., 1999. Mass extinctions and sea-level changes. Earth Science Reviews 48, 217–250.
Hayashi, K.I., Fujisawa, H., Holland, H.D., Ohmoto, H., 1997. Geochemistry of 1.9 Ga sedimentary rocks from northeastern Labrador, Canada. Geochimica et Cosmochimica Acta 61, 4115–4137.
He, B., Xu, Y.G., Chung, S.L., Xiao, L., Wang, Y.M., 2003. Sedimentary evidence for a rapid, kilometer scale crustal doming prior to the eruption of the Emeishan flood basalts. Earth And Planetary Science Letters 213, 391–405.
He, B., Xu, Y.G., Wang, Y.M., Luo, Z.Y., 2006. Sedimentation and lithofacies paleogeography in southwestern China before and after the Emeishan flood volcanism: new insights into surface response to mantle plume activity. Journal of Geology 114, 117–132.
He, B., Xu, Y.G., Huang, X.L., Luo, Z.Y., Shi, Y.R., Yang, Q.J., Yu, S.Y., 2007. Age and duration of the Emeishan flood volcanism, SW China: Geochemistry and SHRIMP zircon U–Pb dating of silicic ignimbrites, post-volcanic Xuanwei Formation and clay tuff at the Chaotian section. Earth And Planetary Science Letters 306–323.
He, B., Xu, Y.G., Campbell, I., 2009. Pre-eruptive uplift in Emeishan ? Nature Geoscience 2, 531–532.
Huang, X.H., 1997. The Lufang rare earth deposit in Weining, western Guizhou and its mineralization. Geology of Guizhou 14, 328–333.
Isozaki, Y., Yao, J.X., Matsuda, T., Sakai, H., Ji, Z.S., Shimizu, N., Kobayashi, N., Kawahata, H., Nishi, H., Takano, M., Kubo, T., 2004. Stratigraphy of the Middle-Upper Permian and Lowermost Triassic at Chaotian, Sichuan, China—record of end-Permian double mass extinction event. Proceedings of the Japan Academy B 80, 10–16.
Isozaki, Y., 2007. Plume winter scenario for biosphere catastrophe: the Permo-Triassic boundary case. In: Yuen, D.A., Maruyama, S., Harato, S., Windley, B.F. (Eds.), Superplume: Beyond Plate Tectonics. Springer, Dordrecht, pp. 409–440.
Isozaki, Y., Ota, A., 2007. Reply to comment by Ali, J.R. and Wignall, P. on Ota, A. and Isozaki, Y., 2006. Fusuline biotic turnover across the Guadalupian–Lopingian (Middle-Upper Permian) boundary in mid-oceanic carbonate buildups: biostratigraphy of accreted limestone, (Japan. Journal of Asian Earth Sciences 26, 353–368). Journal of Asian Earth Science 30, 201–203.
Isozaki, Y., Kawahata, H., Minoshima, K., 2007. The Capitanian (Permian) Kamura cooling event: the beginning of the Paleozoic–Mesozoic transition. Palaeoworld 16, 16–30.
Lai, X.L., Wang, W., Wignall, P.B., Bond, D.P.G., Jiang, H.S., Ali, J.R., John, E.H., Sun, Y.D., 2008. Palaeoenvironmental change during the end-Guadalupian (Permian) mass extinction in Sichuan, China. Palaeogeography, Palaeoclimatology, Palaeoecology 269 (1–2), 78–93.
Li, X.H., Li, Z.X., Zhou, H.W., Liu, Y., Kinny, P.D., 2002. U–Pb zircon geochronology, geochemistry and Nd isotopic study of Neoprozoic bimodal volcanic rocks in the

Kangdian Rift of south China: implications for the initial rifting of Rodinia. Precambrian Research 113, 135–154.
Lopez, J.M.G., Bauluz, B., Fernandez-Nieto, C., Oliete, A.Y., 2005. Factors controlling the trace-element distribution in fine-grained rocks: the Albian kaolinite-rich deposits of the Oliete Basin (NE Spain). Chemical Geology 214, 1–19.
Luo, Z.Y., Xu, Y.G., He, B., Shi, Y.R., Huang, X.L., 2007. Geochronologic and petrochemical evidence for the genetic link between the Maomaogou nepheline syenites and the Emeishan large igneous province. Chinese Science Bulletin 52, 949–958.
Kramer, W., Weatherall, G., Offler, R., 2001. Origin and correlation of tuffs in the Permian Newcastle and Wollombi Coal Measures, NSW, Australia, using chemical fingerprinting. International Journal of Coal Geology 47, 115–135.
Mai, T.N., 1993. The influence of mass and existence form of chemical elements in each weathering zone on their mobility during weathering of igneous rocks. Resource Geology Special Issue 15, 365–372.
Maynard, J.B., 1992. Chemistry of modern soils as a guide to interpreting Precambrian paleosols. The Journal of Geology 100, 279–289.
McLennan, S.M., Nance, W.B., Taylor, S.R., 1980. Rare earth element–thorium correlations in sedimentary rocks, and the composition of the continental crust. Geochimica et Cosmochimica Acta 44, 1833–1839.
Nesbitt, H.W., Wilson, R.E., 1992. Recent chemical-weathering of basalts. American Journal of Science 292, 740–777.
Ota, A., Isozaki, Y., 2006. Fusiline biotic turnover across the Guadalupina–Lopingian (Middle-Upper Permian) boundary in mid-oceanic carbonate build-ups: biostratigraphy of accreted limestone in Japan. Journal of Asian Earth Sciences 26, 353–368.
Sawyer, E.W., 1986. The influence of source rock type, chemical weathering and sorting on the geochemistry of clastic sediments from the Quetico metasedimentary belt, Superior Province, Canada. Chemical Geology 55, 77–95.
Schieber, J., 1992. A combined petrographical–geochemical provenance study of the Newland Formation, Mid-Proterozoic of Montana. Geological Magazine 129, 223–237.
Shellnutt, J.G., Jahn, B.-M., 2010. Formation of the Late Permian Panzhihua plutonic–hypabyssal–volcanic igneous complex: implications for the genesis of Fe–Ti oxide deposits and A-type granites of SW China. Earth and Planetary Science Letters 289, 509–519.
Shellnutt, J.G., Wang, C.Y., Zhou, M.-F., Yang, Y.-H., 2009. Zircon Lu–Hf isotope constraints for A-type granites of the Emeishan large igneous province (SW China): evidence of an enriched mantle source? Journal of Asian Earth Sciences 35, 45–55.
Spears, D.A., Kanaris-Sotiriou, R., 1979. A geochemical and mineralogical investigation of some British and other European tonsteins. Sedimentology 26, 407–425.
Sun, S.S., McDonough, W.F., 1989. Chemical and isotopic systematics of oceanic basalts: implications for mantle composition and processes. In: Saunders, A.D., Norry, M.J. (Eds.), Magmatism in the Ocean Basins: Geological Society London Special Publications, vol. 42, pp. 313–345.
Taylor, S.R., Mclennan, S.M., 1985. The Continental Crust: Its Composition and Evolution. Blackwell, Oxford, UK. 312 pp.
Wang, L.T., Lu, Y.B., Zhao, S.J., Luo, J.H., 1994. Permian Lithofacies Paleogeography and Mineralization in South China. Geological Publishing House, Beijing. (in Chinese with English abstract).
Wignall, P.B., 2001. Large igneous provinces and mass extinctions. Earth Science Reviews 53, 1–33.
Wignall, P.B., Sun, Y.D., Bond, D., Izon, G., Newton, R.J., Vedrine, S., Widdowson, M., Ali, J. R., Lai, X.L., Jiang, H.S., Cope, H., Bottrell, S.H., 2009. Volcanism, mass extinction, and carbon isotope fluctuations in the Middle Permian of China. Science 324, 1179–1182.
Xiao, L., Xu, Y.G., Chung, S.L., He, B., Mei, H.J., 2003. Chemostratigraphic correlation of Upper Permian lavas from Yunnan province, China: extent of the Emeishan large igneous province. International Geology Review 45, 753–766.
Xiao, L., Xu, Y.G., Mei, H.J., Zheng, Y.F., He, B., Pirajno, F., 2004. Distinct mantle sources of low-Ti and high-Ti basalts from the western Emeishan large igneous province, SW China: implications for plume-lithosphere interaction. Earth and Planetary Science Letters 228, 525–546.
Xu, Y.G., Chung, S.L., Jahn, B.M., Wu, G.Y., 2001. Petrologic and geochemical constraints on the petrogenesis of Permian–Triassic Emeishan flood basalts in southwestern China. Lithos 58, 145–168.
Xu, Y.G., Luo, Z.Y., Huang, X.L., He, B., Xiao, L., Xie, L.W., Shi, Y.R., 2008. Zircon U–Pb and Hf isotope constraints on crustal melting associated with the Emeishan mantle plume. Geochimica et Cosmochimica Acta 72, 3084–3104.
Xu, Y.G., Chung, S.L., Shao, H., He, B., 2010. Silicic magmas from the Emeishan large igneous province, Southwest China: petrogenesis and their link with the end-Guadalupian biological crisis. Lithos Emeishan special 119, 47–60.
Zhang, Y.X., Luo, Y.N., Yang, Z.X., 1988. Panxi Rift. Geological Publishing House, Beijing. 466 pp. (Chinese with English abstract).
Zhong, H., Zhu, W.G., 2006. Geochronology of layered mafic intrusions from the Pan-Xi area in the Emeishan large igneous province, SW China. Mineralium Deposita 41, 599–606.
Zhong, H., Zhu, W.G., Chu, Z.Y., He, D.F., Song, X.Y., 2007. Shrimp U–Pb zircon geochronology, geochemistry, and Nd–Sr isotopic study of contrasting granites in the Emeishan large igneous province, SW China. Chemical Geology 236, 112–133.
Zhou, L., Kyte, F.T., 1988. The Permian–Triassic boundary event: a geochemical study of three Chinese sections. Earth And Planetary Science Letters 90, 411–421.
Zhou, M.F., Malpas, J., Song, X.Y., Robinson, P.T., Sun, M., Kennedy, A.K., Lesher, C.M., Keays, R.R., 2002. A temporal link between the Emeishan large igneous province (SW China) and the end-Guadalupian mass extinction. Earth And Planetary Science Letters 196, 113–122.
Zhou, Y., Ren, Y., Bohor, B.F., 1982. Origin and distribution of tonsteins in Late Permian coal seams of southwestern China. International Journal of Coal Geology 2, 49–77.
Zhou, Y.P., 1999. The syn-sedimentary alkaline volcanic ash derived tonsteins of Early Longtan age in southwestern China. Coal geology and exploration 27, 5–9.
Zhou, Y.P., Bohor, B.F., Ren, Y.L., 2000. Trace element geochemistry of altered volcanic ash layers (tonsteins) in Late Permian coal-bearing formations of eastern Yunnan and western Guizhou Provinces, China. International Journal of Coal Geology 44, 305–324.